# RestNet: Boosting Cross-Domain Few-Shot Segmentation with Residual Transformation Network

Xinyang Huang
hsinyanghuang7@gmail.com

Chuang Zhu*
czhu@bupt.edu.com

Wenkai Chen
wkchen@bupt.edu.com

School of Artificial Intelligence,
Beijing University of Posts and
Telecommunications
Beijing, China

**Abstract**

Cross-domain few-shot segmentation (CD-FSS) aims to achieve semantic segmentation in previously unseen domains with a limited number of annotated samples. Although existing CD-FSS models focus on cross-domain feature transformation, relying exclusively on inter-domain knowledge transfer may lead to the loss of critical intra-domain information. To this end, we propose a novel residual transformation network (RestNet) that facilitates knowledge transfer while retaining the intra-domain support-query feature information. Specifically, we propose a Semantic Enhanced Anchor Transform (SEAT) module that maps features to a stable domain-agnostic space using advanced semantics. Additionally, an Intra-domain Residual Enhancement (IRE) module is designed to maintain the intra-domain representation of the original discriminant space in the new space. We also propose a mask prediction strategy based on prototype fusion to help the model gradually learn how to segment. Our RestNet can transfer cross-domain knowledge from both inter-domain and intra-domain without requiring additional fine-tuning. Extensive experiments on ISIC, Chest X-ray, and FSS-1000 show that our RestNet achieves state-of-the-art performance. Our code is available at https://github.com/bupt-ai-cz/RestNet.
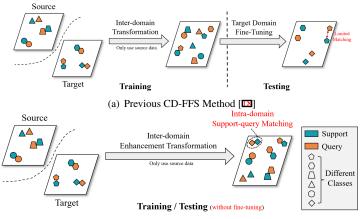
## 1 Introduction

Deep convolutional neural networks (CNNs) have demonstrated remarkable performance in diverse computer vision tasks, including semantic segmentation [24, 29, 43] and object detection [7, 13, 28]. Although CNNs are effective, their dependence on a large number of labeled data is still a constraint. To alleviate this dependence, the Few-shot Semantic Segmentation (FSS) [31] was proposed to learn the model of segmenting new classes with only a few pixel-level annotations. In recent years, significant progress has been made in the FSS [2, 21, 22, 26, 27, 32, 34, 36, 41, 42]. However, it is still challenging to apply them to cross-domain scenarios. To solve this problem, the Cross-Domain Few-Shot Segmentation

*Corresponding author

(a) Previous CD-FFS Method [13]

(b) Our Residual Transformation Network (RestNet)

Figure 1: The comparison between the previous cross-domain few-shot segmentation method and our RestNet. (a) The previous CD-FSS method focused on knowledge transfer using an inter-domain transformation that may lose the intra-domain information, so additional target domain fine-tuning is required. (b) Our RestNet learns knowledge from both inter-domain and intra-domain. It performs cross-domain enhancement transformation while preserving the intra-domain matching information.

(CD-FSS) was proposed [13] to generalize meta-knowledge from the source domain with sufficient labels to the target domain with limited labels.

The CD-FSS problem considers a more realistic scenario: the model cannot access the target data during training, and the data distribution and label space in the test phase are different from those in the training phase. To accomplish the CD-FSS, PATNet [13] was proposed to perform a linear transformation on the support foreground features and query features, project them into domain-agnostic features, and compute the feature similarity in the new spaces before exporting the query mask. However, the cross-domain feature mapping by imprecise projection layers often makes the distribution alignment of features aligned in the original space fail in the new space. In the CD-FSS scenarios, it reflects reduced matching between intra-domain support and query samples, so additional fine-tuning is required in the target domain, as shown in Figure 1(a). In addition, due to the fine-grained differences between support and query samples and the presence of support masks, the learning of knowledge may be biased towards the support samples even if they belong to the same class [40]. To address these problems, we propose the **Res**idual **T**ransformation **Net**work (Rest-Net). It considers not only inter-domain transfer but also the preservation of intra-domain knowledge, as illustrated in Figure 1(b).

For the inter-domain, we propose a novel **S**emantic **E**nhanced **A**nchor **T**ransform (SEAT), which uses the attention to help the model learn advanced semantic features that are then mapped to domain unknown spaces for knowledge migration. Further, we propose a simple and effective **I**ntra-domain **R**esidual **E**nhancement (IRE) mechanism. It associates the information of the original discriminative space to the present domain-agnostic space via residual connection [12] and helps the model to align the support and query features of the domain-agnostic feature space to enhance the intra-domain knowledge representation. The two mechanisms each help the model adapt more comprehensively to cross-domain small-

sample tasks from different perspectives. Finally, we generate a coarse soft query mask and feed it to the network with the support mask through prototype fusion to obtain the final mask, which can help the model learn how to segment step by step.

In summary, our contributions are summarized as follows:

- We propose a Residual Transform network (RestNet) that uses the proposed SEAT and IRE modules to help the model preserve key information in the original domain while performing cross-domain few-shot segmentation.
- We propose a new mask prediction strategy based on the prototype fusion. This strategy helps the proposed RestNet gradually learn how to segment the unseen domain.
- Our method achieves state-of-the-art results on three CD-FSS benchmarks, namely ISIC, Chest X-ray, and FSS-1000. Our RestNet solves the problem of intra-domain knowledge loss under the condition of considering inter-domain knowledge transfer, which provides a new idea for future research in this field.

# 2  Related Work

## 2.1  Domain Adaptive Segmentation

Domain adaptive segmentation has led to some achievements. The goal of the method is to transfer knowledge learned from a labeled source domain to an unlabeled or weakly labeled target domain. The method based on adversarial learning [4, 5, 8, 15] aims to learn domain invariant representations in features. In addition, the design loss function [14, 23, 37] to constrain the data distribution can also achieve feature alignment. These methods operate in settings where the target domain data can be accessed during training to drive model adaption and compensate for domain offsets. In contrast, our source and target domain have completely disjoint label spaces and no target data is required during the CD-FSS training.

## 2.2  Few-Shot Semantic Segmentation

Unlike domain adaptive semantic segmentation, the target domain cannot be accessed by the FSS tasks during training. The goal is to segment new semantic objects in the image, with only a few labeled available. Current methods mainly focus on the improvement of the meta-learning stage. Prototype-based approach [27, 32, 36, 42] is to use methods to extract representative foreground or background prototypes that support data and then use different strategies to interact between different prototypes or between prototypes and query features. Relation-based methods [20, 21, 22, 26, 34, 41] also achieved success in the few-shot segmentation. HSNet [26] uses multi-scale dense matching to construct hypercorrelation and uses 4D convolution to capture context information. RePRI [2] presents a transduction inference for feature extraction on a base class without meta-learning. However, these methods focus only on segmenting new categories from the same domain. Because of the large differences in cross-domain distributions, they cannot be extended to invisible domains.

# 3  Method

## 3.1  Problem Setting

In the problem setting of the CD-FSS, there exists a source domain $(X_s, Y_s)$ and a target domain $(X_t, Y_t)$, where $X$ denotes the distribution of the input data and $Y$ denotes the space
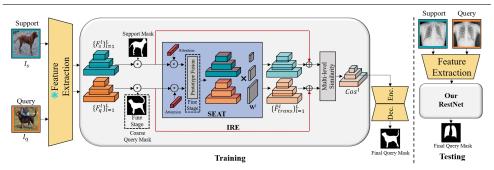
Figure 2: The framework of our RestNet. The model maps support and query features to a new domain-independent space using Semantic Enhanced Anchor Transform (SEAT). The Intra-Domain Residual Enhancement (IRE) module is designed to preserve the matching information of the original feature space in the new space. Next, the similarity between the support and query is calculated and input into the encoder and decoder to generate a rough mask. The final mask is obtained by a prototype fusion mechanism in the fine stage.

of the data label. The input data distribution of the source domain is different from the target domain, and the label space of the source domain does not intersect with the target domain, i.e., $X_s \neq X_t$ and $Y_s \cap Y_t = \emptyset$. The model is trained on the source domain and does not have access to the target data. We place it in a few-shot learning scenario [10] for training and inference based on the episode data $(S, Q)$ as same as the previous work [18]. For the few-shot setup, the support set $S = (I_s^i, M_s^i)_{i=1}^{K}$ contains $K$ image mask pairs, where $I_s^i$ denotes the $i$-th support image and $M_s^i$ denotes the corresponding binary mask. Similarly, the query set is defined as $Q = (I_q^i, M_q^i)_{i=1}^{K}$. In the training or meta-training phase, the model obtains the support set $S$ and the query set $I_q$ from a specific class $c$ as input and predicts the mask $M_q$ of the query image. In the testing or meta-testing phase, the model performance is evaluated by providing the model with the support set and using the query set of the target domain.

## 3.2 Overview

Figure 2 illustrates our RestNet, which incorporates two key components to enable rapid CD-FSS adaptation across both inter- and intra-domain: Semantic Enhancement Anchor Transformation (SEAT) and Intra-domain Residual Enhancement (IRE) module. Given the support set $S = (I_s^i, M_s^i)_{i=1}^{K}$ and the query image $I_q$, we first derive a multi-level feature map by extracting the features of different layers of the shared backbone weights. We map support and query features to a new domain-agnostic space through the semantic enhancement anchor transformation (SEAT). Then, the intra-domain residual enhancement (IRE) module is designed to preserve the matching information of the original feature space in the new feature space. After realignment, we calculate the similarity between the support and query features and input it into the 4D convolution encoder and 2D convolution decoder [26] to generate a coarse query mask. The coarse mask is fed to the network with the support mask through the prototype fusion mechanism to obtain the final mask.

## 3.3 Semantic Enhanced Anchor Transformation

To help the model transfer the cross-domain knowledge, we propose a novel semantic enhancement anchor transformation (SEAT). The goal is to learn a stable pyramid anchor layer using advanced semantic features derived from a unified attention mechanism to translate features into domain-agnostic features. The downstream partitioning module will be easier to predict in such a stable space.

**Semantic Enhancement.** Before the transformation, the quality of segmentation prediction is highly dependent on the quality of advanced features from the encoder. If the encoder fails to provide informative advanced features, it is impossible to obtain useful domain-agnostic features. Thus, we use a unified attention mechanism [58] to enhance the support and query feature semantics at intermediate layer $l$:

$$\hat{\mathbf{F}}^l = \sigma(Conv([\text{AvgPool}(\hat{F}^l); \text{MaxPool}(\hat{F}^l)])) \otimes \hat{F}^l, \tag{1}$$

where $\hat{F}^l$ denotes the masked feature, $\sigma$ denotes the sigmoid function, $[\cdot;\cdot]$ represents the concatenation and $\otimes$ represents the element-wise multiplication. The unified spatial attention mechanism can share an attention extraction module for the feature layers of different feature channels and support-query samples. It can reduce the number of parameters to be learned and help the model learn a unified domain-invariant knowledge between different feature maps from the support and query.

**Anchor Transformation.** Inspired by the previous work [18, 30], we use the linear transformation matrix as the transformation mapper. The matrix can be calculated from the anchor layer parameter matrix and the support prototype. Taking 1-way 1-shot as an example, for the intermediate feature layer $\{F_s^l\}_{l=1}^L$ supporting the image, the $l$-th foreground support prototype is as follows:

$$\mathbf{c}_{s,f}^l = \frac{\sum_i \sum_j F_s^{l,i,j} \psi^l(M_s^{i,j})}{\sum_i \sum_j \psi^l(M_s^{i,j})}, \tag{2}$$

where $\psi^l(\cdot)$ denotes the bilinear interpolation, $F_s^{l,i,j}$ and $M_s^{i,j}$ represent the pixel values corresponding to the support feature and the mask in row $i$ and column $j$ respectively. Similarly, the supporting background prototype $\mathbf{c}_{s,b}^l$ can be obtained in the same way. Therefore, given the weight matrix of anchor layer $\mathbf{A}$, the definition of transformation matrix is as follows:

$$\mathbf{W}\mathbf{C}_s = \mathbf{A}, \tag{3}$$

where $\mathbf{C}_s = \left[\frac{\mathbf{c}_{s,f}}{\|\mathbf{c}_{s,f}\|}, \frac{\mathbf{c}_{s,b}}{\|\mathbf{c}_{s,b}\|}\right]$, $\mathbf{A} = \left[\frac{\mathbf{a}_f}{\|\mathbf{a}_f\|}, \frac{\mathbf{a}_b}{\|\mathbf{a}_b\|}\right]$ and $\mathbf{a}$ is the anchor vector that has the length matching the number of channels in the high-level feature. Therefore, we can calculate the transformation matrix $\mathbf{W}$ conveniently. However, since the prototype $\mathbf{C}_s$ is usually a non-square matrix, we can calculate its generalized inverse [1] with $\mathbf{C}_s^+ = \{\mathbf{C}_s^T \mathbf{C}_s\}^{-1} \mathbf{C}_s^T$. Therefore, the transformation matrix of the $l$-th intermediate layer is calculated as $\mathbf{W}^l = \mathbf{A}^l \mathbf{C}_s^{l+}$. Similar to [18], we have three anchor layers for low, medium, and high-level features respectively. Then, we can map the support and query features to stable domain-agnostic space more effectively through this transformation matrix.

## 3.4 Intra-domain Residual Enhancement

Considering only inter-domain knowledge transfer, the model's ability to perform few-shot tasks in unseen domains is limited. This limitation arises from the fact that the features are

transformed into a unified space solely through an anchor layer, leading to the loss of crucial intra-domain information. This loss is reflected in the reduced matching between support-query features within the same domain. To address this issue, we propose an intra-domain residual enhancement module that leverages residual connections to preserve essential information from the original space to help the model perform well in the unseen domain.

Formally, for the transformed feature $\hat{F}_{trans}^l = \mathbf{W}^l \hat{F}^l$, the definition of intra-domain residual enhancement is as follows:

$$R^l = \hat{F}_{trans}^l \oplus \hat{F}^l, \tag{4}$$

where $\oplus$ denotes the residual connection and $\hat{F}^l$ denotes the masked feature. The residual enhancement module reduces the cross-domain knowledge forgetting caused by anchor layer transformation by introducing support and query information in the original domain. It does not introduce additional parameters or require additional fine-tuning in the target domain.

For each residual enhancement support-query pair, the cosine similarity is calculated to form a 4D hypercorrelation tensor:

$$Cos_{i,j}^l = \text{ReLU}\left( \frac{R_s^l(i) \cdot R_q^l(j)}{\|R_s^l(i)\| \|R_q^l(j)\|} \right), \tag{5}$$

where $R_s^l(i)$ and $R_q^l(j)$ means the $i$-th support and $j$-th query residual enhancement feature. The similarity is fed to the 4D convolution encoder and the 2D convolution decoder to generate the query mask. The prediction query mask and the ground truth mask are used to calculate the cross-entropy loss, and the model parameters are updated by backpropagation.

## 3.5  Mask Prediction Strategy

Due to the fine-grained difference between the support query samples and the lack of the query mask, the learning of knowledge may also be biased towards the support samples [40]. At the same time, we can not calculate the query prototype, resulting in the transformation matrix being biased toward the support. To solve the above problems, we use the idea of coarse to fine [25] to generate a coarse query mask, and then feed it and the support mask to the network through the prototype fusion mechanism to get the final prediction mask.

Specifically, the model first generates a coarse soft mask $\hat{M}_q$ for query samples, and the query foreground mask is calculated as follows:

$$\hat{\mathbf{c}}_{q,f}^l = \frac{\sum_i \sum_j F_q^{l,i,j} \psi^l(\hat{M}_q^{i,j})}{\sum_i \sum_j \psi^l(\hat{M}_q^{i,j})}, \tag{6}$$

where $F_q^{l,i,j}$ and $\hat{M}_q^{i,j}$ represent the pixel values corresponding to the query feature and the soft mask respectively. The background mask for the query can also be calculated in the same way. Then we use a simple prototype fusion mechanism to get the final unbiased prototype:

$$\mathbf{c}_f^l = \alpha \mathbf{c}_{s,f}^l + (1-\alpha)\hat{\mathbf{c}}_{q,f}^l, \tag{7}$$

where $\alpha$ is a learnable parameter. Bring the fused prototype into Equation 3 to get the exact transformation matrix and go through subsequent modules to get the final query mask. This method not only solves the potential phenomenon of supporting sample over-fitting in FSS but also helps the model learn how to segment across domains step by step. Finally, we optimize the whole model through the cross-entropy loss.

Table 1: The results of comparison with FSS and CD-FSS methods under 1-way 1-shot and 5-shot settings on the CD-FSS benchmark. It is noteworthy that all methods are trained in PASCAL VOC and tested on the CD-FSS benchmark.

| Methods | Backbone | ISIC | | Chest X-ray | | FSS-1000 | | Average | |
|---|---|---|---|---|---|---|---|---|---|
| | | 1-shot | 5-shot | 1-shot | 5-shot | 1-shot | 5-shot | 1-shot | 5-shot |
| Few-shot Segmentation Methods | | | | | | | | | |
| AMP [__] | VGG-16 | 28.42 | 30.41 | 51.23 | 53.04 | 57.18 | 59.24 | 45.61 | 47.56 |
| PGNet [__] | ResNet-50 | 21.86 | 21.25 | 33.95 | 27.96 | 62.42 | 62.74 | 39.41 | 37.32 |
| PANet [__] | ResNet-50 | 25.29 | 33.99 | 57.75 | 69.31 | 69.15 | 71.68 | 50.73 | 58.33 |
| CaNet [__] | ResNet-50 | 25.16 | 28.22 | 28.35 | 28.62 | 70.67 | 72.03 | 41.39 | 42.96 |
| RPMMs [__] | ResNet-50 | 18.02 | 20.04 | 30.11 | 30.82 | 65.12 | 67.06 | 37.75 | 39.31 |
| PFENet [__] | ResNet-50 | 23.50 | 23.83 | 27.22 | 27.57 | 70.87 | 70.52 | 40.53 | 40.64 |
| RePRI [__] | ResNet-50 | 23.27 | 26.23 | 65.08 | 65.48 | 70.96 | 74.23 | 53.10 | 55.31 |
| HSNet [__] | ResNet-50 | 31.20 | 35.10 | 51.88 | 54.36 | 77.53 | 80.99 | 53.54 | 56.82 |
| Cross-domain Few-shot Segmentation Methods | | | | | | | | | |
| PATNet [__] | VGG-16 | 33.07 | 45.83 | 57.83 | 60.55 | 71.60 | 76.17 | 54.17 | 60.85 |
| RestNet (Ours) | VGG-16 | 37.00 | 43.10 | 62.03 | 62.41 | 75.20 | 78.81 | 58.08 | 61.44 |
| PATNet [__] | ResNet-50 | 41.16 | **53.58** | 66.61 | 70.20 | 78.59 | 81.23 | 62.12 | 68.34 |
| RestNet (Ours) | ResNet-50 | **42.25** | 51.10 | **70.43** | **73.69** | **81.53** | **84.89** | **64.74** | **69.89** |

# 4 Experiments

## 4.1 Implementation Details

Following the previous approach, we used PASCAL VOC 2012 [9] and SBD [11] as training domains, and then tested our models on ISIC [6, 35], Chest X-ray [4, 16], and FSS-1000 [19], respectively. Each run contains 1200 tasks that contain all datasets except FSS-1000. FSS-1000 has 2400 tasks per run [18]. We chose VGG-16 [33] and ResNet-50 [12] for feature extraction. During the training, we kept these weights frozen and selected the feature map as the same as the previous work [18]. We employed Adam [17] as the optimizer with a learning rate of 1e-3.

## 4.2 Experimental Results

As shown in Table 1, our average results at 1-shot and 5-shot show that compared to existing methods, the mIOU of VGG-16 has increased by 3.91% and 0.59%, and the mIOU of ResNet-50 has increased by 2.62% and 1.55%. In the case of a large gap between the fields in the source domain dataset, our model achieves SOTA in all results for Chest X-rays. In ISIC, the mIOU of VGG-16 increased by 3.93% (1-shot), and the mIOU of ResNet-50 increased by 1.09% (1-shot). For FSS-1000, which has a relatively small gap from the source domain dataset, our model surpasses all existing methods and validates its advantages in CD-FSS. In addition, we show some qualitative results of the proposed method on different datasets in Figure 3. These results prove that our method can improve the generalization ability, which benefits from that our method can learn cross-domain knowledge from different views.

## 4.3 Ablation Study

### 4.3.1 Component Analysis

Our method mainly includes three parts, namely the Semantic Enhanced Anchor Transformation (SEAT) module and the Residual Enhancement (IRE) module, and Mask Prediction Strategy (MPS). We validated the effectiveness of each component and presented the results
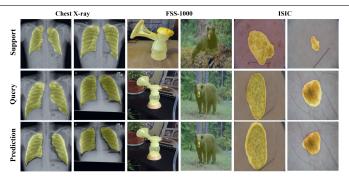
Figure 3: Qualitative results of our model for 1-way 1-shot in different CD-FSS datasets. The model is trained using PASCAL VOC. Best color view and zoom in.

in Table 2. It can be concluded that SEAT and IRE have brought significant improvements to the model from different perspectives, and MPS is also indispensable.

### 4.3.2 Effect of Different Attention

We mentioned a unified attention mechanism in Section 3.3. In Table 3, we calculated its results on the FSS-1000 with different attention mechanisms (i.e., support and query non-shared attention mechanism modules). The results show that a unified attention mechanism can not only help the model reduce learnable parameters but also help the model learn unified support query attention information to achieve better segmentation results.

Table 2: Ablation study of key modules on FSS-1000.

| Baseline | SEAT | IRE | MPS | 1-shot mIOU |
|----------|------|-----|-----|-------------|
| ✓ | | | | 77.53 |
| ✓ | ✓ | | | 78.21 |
| ✓ | ✓ | ✓ | | 81.03 |
| ✓ | ✓ | ✓ | ✓ | **81.53** |

Table 3: Ablation study of different attention on FSS-1000.

| Method | 1-shot mIOU |
|--------|-------------|
| Different Attention | 81.69 |
| Unified Attention | **82.03** |

## 4.4 Additional Analysis

### 4.4.1 Visualization of Intra-domain Knowledge

In Section 3.4, we mentioned the importance of intra-domain matching similarity. To quantify this attribute, for the same domain support and query samples, we calculate the support-query similarity in Equation 5 and count the pixel pairs in each similarity whose value is greater than zero. We call these pixel pairs *intra-domain active matching*. The Intra-domain active matching reflects the knowledge learning between support and query samples from the same domain, which can well represent the retention of intra-domain knowledge by the model after cross-domain feature projection in the CD-FSS.

Specifically, we visualized the active matching of our method and existing methods [18] during the training process, as shown in Figure 4(a), where *Original* denotes no feature transformation. Compared to existing methods, our method can well preserve the intra-domain
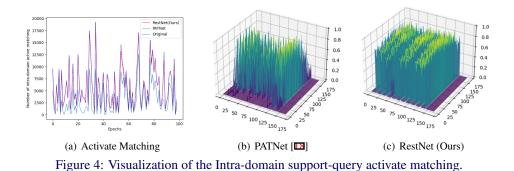
| (a) Activate Matching | (b) PATNet [13] | (c) RestNet (Ours) |

Figure 4: Visualization of the Intra-domain support-query activate matching.

Table 4: Comparison of the number of additional parameters of different methods.

| Method | HSNet [22] | PATNet [13] | RestNet (Ours) |
|---|---|---|---|
| Additional Parameters (M) | 2.5740 M | 2.5809 M | 2.5812 M |

knowledge in the original space and reduce the loss caused by cross-domain transformation. Further, we visualize the support-query similarity for the 30th epoch. For ease of visualization, we reshape the similarity from $\mathbb{R}^{\in H \times W \times H \times W}$ to $\mathbb{R}^{\in HW \times HW}$, as shown in Figure 4(b) and Figure 4(c). It can be shown that our method can activate more intra-domain matching, helping the model utilize more intra-domain support-query information.

### 4.4.2 Comparison of Model Parameter Quantities

In Table 4, we compare the number of parameters with those of existing FSS methods and CD-FSS methods. We calculate the number of additional parameters relative to the backbone. The results show that our method only introduces a very small number of parameters but has additional performance improvements compared with the recent CD-FSS method.

## 5 Conclusion

In this work, we propose a residual transform network (RestNet) to solve the cross-domain few-shot segmentation (CD-FSS). It is to comprehensively help the model to transfer knowledge with few samples from both inter-domain and intra-domain perspectives. To achieve this, we propose a Semantic Enhanced Anchor Transformation (SEAT) module to help the model learn domain-independent features using advanced semantic features. In addition, an intra-domain residual enhancement (IRE) module is also involved to help the model enhance intra-domain information while transferring knowledge between domains. Finally, we use the mask prediction strategy based on prototype fusion to help the model gradually learn how to segment the unseen domain. On the three CD-FSS benchmarks, several experiments have proved that our RestNet achieves state-of-the-art performance.

# Acknowledgement

# References

[1] Adi Ben-Israel and Thomas NE Greville. *Generalized inverses: theory and applications*, volume 15. Springer Science & Business Media, 2003.

[2] Malik Boudiaf, Hoel Kervadec, Ziko Imtiaz Masud, Pablo Piantanida, Ismail Ben Ayed, and Jose Dolz. Few-shot segmentation without meta-learning: A good transductive inference is all you need? In *Proceedings of the IEEE/CVF Conference on Computer Vision and Pattern Recognition*, pages 13979–13988, 2021.

[3] Sema Candemir, Stefan Jaeger, Kannappan Palaniappan, Jonathan P Musco, Rahul K Singh, Zhiyun Xue, Alexandros Karargyris, Sameer Antani, George Thoma, and Clement J McDonald. Lung segmentation in chest radiographs using anatomical atlases with nonrigid registration. *IEEE transactions on medical imaging*, 33(2):577–590, 2013.

[4] Yi-Hsin Chen, Wei-Yu Chen, Yu-Ting Chen, Bo-Cheng Tsai, Yu-Chiang Frank Wang, and Min Sun. No more discrimination: Cross city adaptation of road scene segmenters. In *Proceedings of the IEEE International Conference on Computer Vision*, pages 1992–2001, 2017.

[5] Yuhua Chen, Wen Li, and Luc Van Gool. Road: Reality oriented adaptation for semantic segmentation of urban scenes. In *Proceedings of the IEEE conference on computer vision and pattern recognition*, pages 7892–7901, 2018.

[6] Noel Codella, Veronica Rotemberg, Philipp Tschandl, M Emre Celebi, Stephen Dusza, David Gutman, Brian Helba, Aadi Kalloo, Konstantinos Liopyris, Michael Marchetti, et al. Skin lesion analysis toward melanoma detection 2018: A challenge hosted by the international skin imaging collaboration (isic). *arXiv preprint arXiv:1902.03368*, 2019.

[7] Jifeng Dai, Haozhi Qi, Yuwen Xiong, Yi Li, Guodong Zhang, Han Hu, and Yichen Wei. Deformable convolutional networks. In *Proceedings of the IEEE international conference on computer vision*, pages 764–773, 2017.

[8] Liang Du, Jingang Tan, Hongye Yang, Jianfeng Feng, Xiangyang Xue, Qibao Zheng, Xiaoqing Ye, and Xiaolin Zhang. Ssf-dan: Separated semantic feature based domain adaptation network for semantic segmentation. In *Proceedings of the IEEE/CVF International Conference on Computer Vision*, pages 982–991, 2019.

[9] Mark Everingham, Luc Van Gool, Christopher KI Williams, John Winn, and Andrew Zisserman. The pascal visual object classes (voc) challenge. *International journal of computer vision*, 88:303–308, 2009.

[10] Chelsea Finn and Sergey Levine. Meta-learning and universality: Deep representations and gradient descent can approximate any learning algorithm. *arXiv preprint arXiv:1710.11622*, 2017.

[11] Bharath Hariharan, Pablo Arbeláez, Lubomir Bourdev, Subhransu Maji, and Jitendra Malik. Semantic contours from inverse detectors. In *2011 international conference on computer vision*, pages 991–998. IEEE, 2011.

[12] Kaiming He, Xiangyu Zhang, Shaoqing Ren, and Jian Sun. Deep residual learning for image recognition. In *Proceedings of the IEEE conference on computer vision and pattern recognition*, pages 770–778, 2016.

[13] Kaiming He, Georgia Gkioxari, Piotr Dollár, and Ross Girshick. Mask r-cnn. In *Proceedings of the IEEE international conference on computer vision*, pages 2961–2969, 2017.

[14] Joy Hsu, Wah Chiu, and Serena Yeung. Darcnn: Domain adaptive region-based convolutional neural network for unsupervised instance segmentation in biomedical images. In *Proceedings of the IEEE/CVF Conference on Computer Vision and Pattern Recognition*, pages 1003–1012, 2021.

[15] Jiaxing Huang, Dayan Guan, Aoran Xiao, and Shijian Lu. Multi-level adversarial network for domain adaptive semantic segmentation. *Pattern Recognition*, 123:108384, 2022.

[16] Stefan Jaeger, Alexandros Karargyris, Sema Candemir, Les Folio, Jenifer Siegelman, Fiona Callaghan, Zhiyun Xue, Kannappan Palaniappan, Rahul K Singh, Sameer Antani, et al. Automatic tuberculosis screening using chest radiographs. *IEEE transactions on medical imaging*, 33(2):233–245, 2013.

[17] Diederik P Kingma and Jimmy Ba. Adam: A method for stochastic optimization. *arXiv preprint arXiv:1412.6980*, 2014.

[18] Shuo Lei, Xuchao Zhang, Jianfeng He, Fanglan Chen, Bowen Du, and Chang-Tien Lu. Cross-domain few-shot semantic segmentation. In *Computer Vision–ECCV 2022: 17th European Conference, Tel Aviv, Israel, October 23–27, 2022, Proceedings, Part XXX*, pages 73–90. Springer, 2022.

[19] Xiang Li, Tianhan Wei, Yau Pun Chen, Yu-Wing Tai, and Chi-Keung Tang. Fss-1000: A 1000-class dataset for few-shot segmentation. In *Proceedings of the IEEE/CVF conference on computer vision and pattern recognition*, pages 2869–2878, 2020.

[20] Yiwen Li, Gratianus Wesley Putra Data, Yunguan Fu, Yipeng Hu, and Victor Adrian Prisacariu. Few-shot semantic segmentation with self-supervision from pseudo-classes. In *32nd British Machine Vision Conference 2021, BMVC 2021, November 22-25, 2021*, 2021.

[21] Jie Liu, Yanqi Bao, Wenzhe Yin, haochen wang, Yang Gao, Jan-Jakob Sonke, and Efstratios Gavves. Few-shot semantic segmentation with support-induced graph convolutional network. In *33rd British Machine Vision Conference 2022, BMVC 2022, London, UK, November 21-24, 2022*. BMVA Press, 2022. URL https://bmvc2022.mpi-inf.mpg.de/0126.pdf.

[22] Weide Liu, Chi Zhang, Guosheng Lin, and Fayao Liu. Crnet: Cross-reference networks for few-shot segmentation. In *Proceedings of the IEEE/CVF Conference on Computer Vision and Pattern Recognition*, pages 4165–4173, 2020.

[23] Yuang Liu, Wei Zhang, and Jun Wang. Source-free domain adaptation for semantic segmentation. In *Proceedings of the IEEE/CVF Conference on Computer Vision and Pattern Recognition*, pages 1215–1224, 2021.

[24] Jonathan Long, Evan Shelhamer, and Trevor Darrell. Fully convolutional networks for semantic segmentation. In *Proceedings of the IEEE conference on computer vision and pattern recognition*, pages 3431–3440, 2015.

[25] David Marr. *Vision: A computational investigation into the human representation and processing of visual information*. MIT press, 2010.

[26] Juhong Min, Dahyun Kang, and Minsu Cho. Hypercorrelation squeeze for few-shot segmentation. In *Proceedings of the IEEE/CVF international conference on computer vision*, pages 6941–6952, 2021.

[27] Atsuro Okazawa. Interclass prototype relation for few-shot segmentation. In *Computer Vision–ECCV 2022: 17th European Conference, Tel Aviv, Israel, October 23–27, 2022, Proceedings, Part XXIX*, pages 362–378. Springer, 2022.

[28] Joseph Redmon, Santosh Divvala, Ross Girshick, and Ali Farhadi. You only look once: Unified, real-time object detection. In *Proceedings of the IEEE conference on computer vision and pattern recognition*, pages 779–788, 2016.

[29] Olaf Ronneberger, Philipp Fischer, and Thomas Brox. U-net: Convolutional networks for biomedical image segmentation. In *Medical Image Computing and Computer-Assisted Intervention–MICCAI 2015: 18th International Conference, Munich, Germany, October 5-9, 2015, Proceedings, Part III 18*, pages 234–241. Springer, 2015.

[30] Jun Seo, Young-Hyun Park, Sung Whan Yoon, and Jaekyun Moon. Task-adaptive feature transformer with semantic enrichment for few-shot segmentation. *arXiv preprint arXiv:2202.06498*, 2022.

[31] Amirreza Shaban, Shray Bansal, Zhen Liu, Irfan Essa, and Byron Boots. One-shot learning for semantic segmentation. *arXiv preprint arXiv:1709.03410*, 2017.

[32] Mennatullah Siam, Boris N Oreshkin, and Martin Jagersand. Amp: Adaptive masked proxies for few-shot segmentation. In *Proceedings of the IEEE/CVF International Conference on Computer Vision*, pages 5249–5258, 2019.

[33] Karen Simonyan and Andrew Zisserman. Very deep convolutional networks for large-scale image recognition. *arXiv preprint arXiv:1409.1556*, 2014.

[34] Zhuotao Tian, Hengshuang Zhao, Michelle Shu, Zhicheng Yang, Ruiyu Li, and Jiaya Jia. Prior guided feature enrichment network for few-shot segmentation. *IEEE transactions on pattern analysis and machine intelligence*, 44(2):1050–1065, 2020.

[35] Philipp Tschandl, Cliff Rosendahl, and Harald Kittler. The ham10000 dataset, a large collection of multi-source dermatoscopic images of common pigmented skin lesions. *Scientific data*, 5(1):1–9, 2018.

[36] Kaixin Wang, Jun Hao Liew, Yingtian Zou, Daquan Zhou, and Jiashi Feng. Panet: Few-shot image semantic segmentation with prototype alignment. In *proceedings of the IEEE/CVF international conference on computer vision*, pages 9197–9206, 2019.

[37] Wenguan Wang, Tianfei Zhou, Fisher Yu, Jifeng Dai, Ender Konukoglu, and Luc Van Gool. Exploring cross-image pixel contrast for semantic segmentation. In *Proceedings of the IEEE/CVF International Conference on Computer Vision*, pages 7303–7313, 2021.

[38] Sanghyun Woo, Jongchan Park, Joon-Young Lee, and In So Kweon. Cbam: Convolutional block attention module. In *Proceedings of the European conference on computer vision (ECCV)*, pages 3–19, 2018.

[39] Boyu Yang, Chang Liu, Bohao Li, Jianbin Jiao, and Qixiang Ye. Prototype mixture models for few-shot semantic segmentation. In *Computer Vision–ECCV 2020: 16th European Conference, Glasgow, UK, August 23–28, 2020, Proceedings, Part VIII 16*, pages 763–778. Springer, 2020.

[40] Zican Zha, Hao Tang, Yunlian Sun, and Jinhui Tang. Boosting few-shot fine-grained recognition with background suppression and foreground alignment. *IEEE Transactions on Circuits and Systems for Video Technology*, 2023.

[41] Chi Zhang, Guosheng Lin, Fayao Liu, Jiushuang Guo, Qingyao Wu, and Rui Yao. Pyramid graph networks with connection attentions for region-based one-shot semantic segmentation. In *Proceedings of the IEEE/CVF International Conference on Computer Vision*, pages 9587–9595, 2019.

[42] Chi Zhang, Guosheng Lin, Fayao Liu, Rui Yao, and Chunhua Shen. Canet: Class-agnostic segmentation networks with iterative refinement and attentive few-shot learning. In *Proceedings of the IEEE/CVF Conference on Computer Vision and Pattern Recognition*, pages 5217–5226, 2019.

[43] Hengshuang Zhao, Jianping Shi, Xiaojuan Qi, Xiaogang Wang, and Jiaya Jia. Pyramid scene parsing network. In *Proceedings of the IEEE conference on computer vision and pattern recognition*, pages 2881–2890, 2017.